ELSEVIER

Chemical Engineering Science 62 (2007) 339–355

Chemical Engineering Science

www.elsevier.com/locate/ces

Experimental study of inlet phenomena of 35° inclined non-aerated and aerated Y-inlets in a dilute cold-flow riser

G. Van engelandt, J. De Wilde[1], G.J. Heynderickx*, G.B. Marin

Laboratory for Petrochemical Engineering, Ghent University, Krijgslaan 281 (S5), B-9000 Ghent, Belgium

Available online 9 September 2006

Abstract

Inlet phenomena in a 0.1 m diameter cold-flow riser with a 35° inclined side inlet are studied experimentally using 3D-Laser Doppler Anemometry for solids fluxes of 0.5–4.5 $kg/m^2/s$ and gas velocities of 5.3–7.4 m/s. In the vicinity of the solids inlet, radial gas-solids mixing is hindered and bypassing of the solids jet occurs, resulting in steep velocity gradients and off-centre maxima in the velocity field. The feeding conditions and the type of the solids affect the bottom operation and gas–solids mixing to a large extent: compared to FCC particles, silica particles extend the acceleration zone in the riser. Low gas flow rates and/or high solids feeding rates result in an increased penetration depth of the solids jet and in explicit bypass zones in the plane facing the inlet. High root mean square fluctuating particle velocities are observed at the solids jet boundaries. A non-aerated Y-inlet configuration causes vortex formation, inducing a small reflux into the upper dilute part of the standpipe. The influence of dilution of the inlet solids jet is also investigated using an "aerated" inlet configuration. Aerated inlets lead to better entrainment, improved radial mixing, less pronounced broader bypass zones and a firm reduction of the penetration depth. In the 0.1 m diameter riser, radial mixing quickly dissipates the non-uniformities introduced by the solids inlet. Reflection phenomena can, however, occur in the case of a non-aerated solids inlet.

Keywords: Circulating fluidized bed; Riser; Gas–solid flow; Laser Doppler Anemometry; Inlet phenomena; Y-inlet

1. Introduction

Circulating fluidized bed (CFB) reactors or riser reactors are interesting for application in large scale processes of the (petrochemical) industry, as for example, fluid catalytic cracking (FCC, Das et al., 2003) or the SO_2–NO_x adsorption process (SNAP, Das et al., 2001). Riser reactors allow a continuous operation and offer advantages with respect to mass and heat transfer. The overall efficiency of a riser is improved when a uniform distribution of the solid particles is obtained. At high solids fluxes and/or low gas velocities (that is operating conditions at which most of the CFB reactors are operated), radial uniformity is disturbed by lateral segregation and backmixing phenomena resulting in core-annulus flow. Moreover, axial segregation phenomena result in a distinctive dilute transport zone in the upper part and a dense fast fluidized zone in the bottom part of the riser.

Uniformity over the entire riser height is greatly influenced by inlet and outlet effects (De Wilde et al., 2003a,b, 2005). Although there are a large number of papers reporting on riser hydrodynamics only a few of them are dealing with the influence of inlet geometries. Experimental data on inlet geometries are hardly available (Cheng et al., 1998). Realistic inlet configurations are difficult to study because the introduction of the particles in the system is usually abrupt, resulting in steep gradients in the particle concentration and velocity profiles.

Arastoopour (2001a) simulated the flow of gas and solids in both a horizontal and a 45° inclined inlet configuration. The main focus of the study was on the flow pattern in the solids feeding channel to the riser. The simulations showed that within the horizontal inlet channel, the solids accumulated at the bottom of the channel prior to their entry into the riser. Local gas aeration and inclination of the solids inlet to 45° resulted in less

* Corresponding author. Tel.: +32 9 264 45 16; fax: +32 9 264 49 99.
E-mail address: geraldine.heynderickx@ugent.be (G.J. Heynderickx).
[1] Currently at: Department of Materials and Process Engineering (IMAP), Université catholique de Louvain (UCL), Belgium.

0009-2509/$ - see front matter © 2006 Elsevier Ltd. All rights reserved.
doi:10.1016/j.ces.2006.08.072

accumulation in the solids inlet channel and in a more uniform solids entry in the riser.

In the Fluor Daniel plenary lecture, Arastoopour (2001b) presented 3D simulations of a 0.2 m diameter, 14.2 m tall riser (489 $kg/m^2/s$ solids flux) with a single inlet–outlet configuration similar to the Knowlton et al. (1995) experimental set-up and investigated the influence of the angular position of a side solids inlet (45°, 90° and 135° inclined). The simulations showed that the solids mass flux profiles are asymmetric and that the shape of these profiles depends on the angular positions of the inlet. Moreover, it was shown that big clusters of solids moving downwards force the gas to move through different radial positions in the riser. Arastoopour (2001b) indicated the need for detailed experimental measurements near the riser inlets and outlets and stated that better gas–solids mixing at the entrance would create better mixing throughout the whole riser.

2D simulations by Benyahia et al. (2000) related with the Knowlton et al. (1995) experiment (0.2 m diameter, 14.2 m tall riser, 489 $kg/m^2/s$ solids flux) showed that a one-sided inlet geometry (45° inclination) could lead to bypass, resulting in a limited gas–solids mixing over the entire height of the riser and causing the typical core-annular flow regime in the riser to disappear. The simulated flow field was asymmetric with most of the particles accumulating near the inlet side of the riser. The calculated asymmetric profiles were verified with experimental data (Knowlton et al., 1995) that were taken from one wall to the centre line of the riser only, so that asymmetry in the experimental profiles could not be verified. The authors emphasize the need for 3D experimentation and implementation of the real inlet and outlet configurations and conditions to accurately simulate and validate in- and outlet effects.

Shadle et al. (2001) argue that 2D simulations can overestimate the recirculation rate of the solids near the in- and outlet zones due to the reduced spatial degrees of freedom in 2D for the flow to bypass obstructions (clusters, streamers, solids jets). 3D simulations improved the accuracy of the simulations and showed a reduction of the strong back mixing near the in- and outlet zones.

In the present work the effects of a 35° inclined Y-inlet geometry and of the operating conditions on the flow pattern in a dilute phase cold-flow riser are studied both qualitatively and quantitatively using 3D-Laser Doppler Anemometry (LDA). The main goal is to provide accurate quantitative 3D data in the inlet and acceleration zone of the riser, allowing to validate models and CFD codes used for 3D simulations, in particular the FLOW-MER code developed at the Laboratorium voor Petrochemische Techniek (LPT) (De Wilde, 2000; De Wilde et al., 2003b, 2005). Due to the acceleration, data from near a side solids inlet contain more information than data from the fully developed zone and are particularly suited for model and code validation.

2. Experimental set-up: the LPT cold-flow pilot riser

Fig. 1 shows a schematic representation of the experimental cold-flow pilot scale riser (Van engelandt et al., 2004). The set-up (Fig. 1, left) mainly consists of a 8.765 m high pyrex glass cylindrical riser (1–5), inner diameter $\phi = 0.1$ m, a 4 m high fluidized bed (11,13), $\phi = 0.3$ m, and a 2 m long aerated standpipe (8, 9), $\phi = 0.08$ m. Two high efficiency glass cyclones (24) $\phi = 0.3$ m and (25) $\phi = 0.225$ m (connected to the fluidized bed by means of diplegs (15, 16, 17, 19)) and a bag filter (26) with 15 μm cut diameter guarantee a good recuperation of solids from the air flow through the riser. Additionally, a high efficiency glass cyclone ($\phi = 0.15$ m is connected to the outlet (18) of the fluidized bed (11, 13), recuperating the entrained particles from the fluidized bed by means of a dipleg (12, 14). In order to measure the total solids mass flow in the riser, the recirculation loop also includes a quick closing valve (27). Valve (27) locks the return leg of the primary and secondary cyclone and a part of the cylone dipleg tube (16) will get filled, as in a weighing unit. The solids flux (0–400 $kg/m^2/s$) is mechanically controlled by means of a diaphragm valve (23). The solids (FCCU-E catalyst (Engelhard corp.), mean volume averaged diameter 77 μm and solids density 1550 kg/m^3, particle size distribution given in Table 1), are injected via an asymmetric Y-shaped side inlet (22) which is inclined 35° with the vertical *Z*-axis in the *YZ* plane (Fig. 1, middle). The solids inlet ($\phi = 0.08$ m) is located 0.5 m above the gas inlet and is positioned 51° counter-clock-wise of the outlet in the *YZ* plane, near the right side wall at $R = 0.05$ m (Fig. 1, middle). The air inlet (21), $\phi = 0.05$ m, expanding to $\phi = 0.1$ m, makes a 90° angle with both the *Z*-axis and the *Y*-axis (aligned with the *X*-axis) and is located in the *XZ* plane. Air is deliveredby a 90 kW screw compressor (free air delivery 1000 Nm^3/h, pressurized tank at 4 bar). Dry air coming from the compressor (20–30% relative humidity (RH)) is moistened with steam (0–10 kg/h) to 50–60% RH in order to minimize static electricity effects. The air flow in the riser is measured with a vortex flow meter and in the fluidized bed by a swirl flow meter. Moreover, various aeration taps (1 m^3/h) in the return legs supply extra air, in order to avoid defluidization in the cyclone diplegs (14, 15) and in the standpipe (9) (see Fig. 1, right). The volumetric flow rate of the air is measured with rotameters.

A 3D LDA is used for measuring 3D local mean and fluctuating particle velocities under dilute phase conditions. The LDA measurement technique has its limitations: in a region of high solids volume fractions (say 3%), light scattering from particles outside the measuring volume and blockage of the laser light become significant and result in a considerable decrease of the data rate and in unreliable noisy data. This is especially the case in inlet (and outlet) zones where particle interaction with the wall is very intensive and results in the formation of opaque dense zones that are hard to penetrate by the laser beams. A possible technique to eliminate the blocking effect is to match the index of refraction of some of the solid particles to the fluid. Alternatively, the LDA measurements should become invasive, with an evident distortion of the flow patterns, severely affecting the accuracy of the experiments. For the reasons mentioned above, the measurements with a significant data rate (> 200#/s) and allowing an acceptable accuracy of 1–5% are only possible using inlet jets that result in a maximum overall solids fraction of 0.3% downstream in the riser.

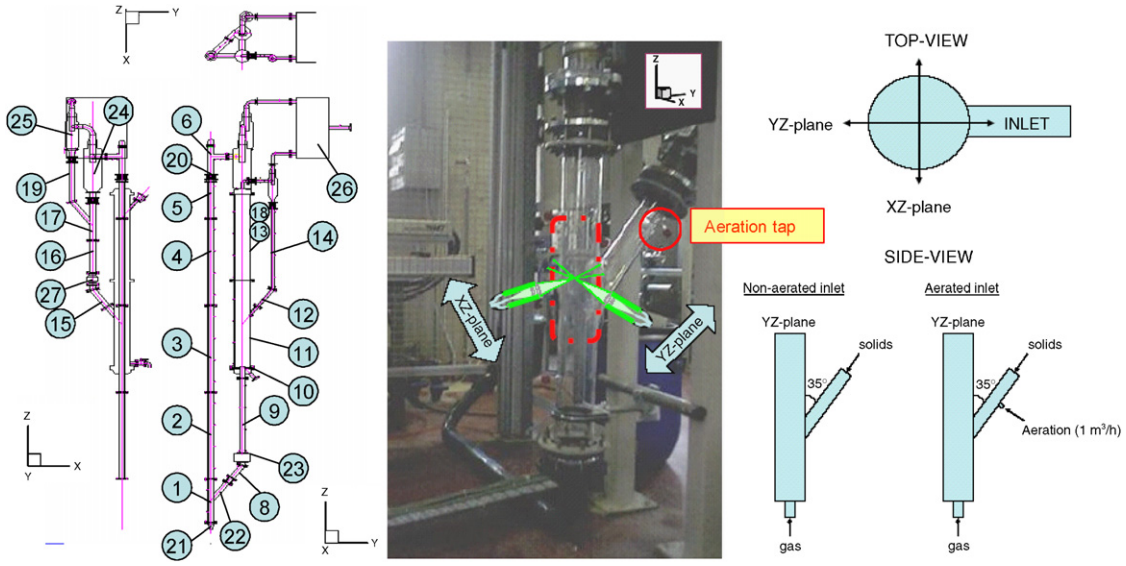

Fig. 1. Schematic representation of the cold-flow pilot installation for hydrodynamic research of gas solids flow in risers at the LPT: detail of the riser inlet section.

The experiments shown in this paper are under SNAP (De Wilde, 2000; Das et al., 2001) conditions ($\varepsilon_s < 0.00075$), i.e., low inlet solids fluxes between 0.5 and 4.5 $kg/m^2/s$ in the riser. The SNAP process, developed by FLS-Miljø (DK), in which simultaneous adsorption of SO_2 and NO_x on Na-g Al_2O_3 takes place in a dilute phase riser reactor (De Wilde, 2000; Das et al., 2001). The dilute operating conditions allow the use of LDA as an appropriate and accurate measuring technique. Furthermore, the dilute operating conditions allow gas solid flow model validation. With the computationally affordable meshes, the currently available Eulerian–Eulerian gas–solid flow models need to be adapted for denser gas–solid flow conditions (higher than 100 $kg/m^2/s$) to account for the presence of meso-scale structures, i.e., clusters and streamers, of which the behaviour is not explicitly calculated (Agrawal et al., 2001; Zhang and Vander-Heyden, 2002; Heynderickx et al., 2004). Because of the computational load, high resolution meshes cannot be used for the calculation of industrial size risers. The development of solid phase subgrid-scale models should overcome this problem in the near future (Cheng et al., 1999; Zheng et al., 2001). As the size of a cluster and the probability of its formation decrease with increasing gas velocity and decreasing solid flux, the calculations and the validation experiments in this paper, are limited to dilute conditions (solid flux 4.5 $kg/m^2/s$) where cluster formation is limited.

The LDA system allows highly accurate measurements with large spatial and temporal resolution: the uncertainty of the measured mean velocities is < 1–2% and of the measured RMS velocities < 5% with a total of 3000 validated signals.

3. Experimental study of the inlet effects of a 35° Y-shaped side inlet

Conditions for the experimental study are summarized in Table 1. The experimental solids mass flow rate is, respectively, 0.003925, 0.02355 and 0.035325 kg/s, corresponding to solids fluxes of 0.5, 3 and 4.5 $kg/m^2/s$ in the riser. The gas flow rates are 150, 180 and 210 m^3/h, corresponding to 5.3, 6.4 and 7.4 m/s superficial gas velocity in the riser. These are typical operating conditions for the SNAP process (De Wilde, 2000; Das et al., 2001). It should be noted that under these dilute conditions the solids enter the riser as a dense solids jet in which ε_s approaches the packing limit (solids volume fraction = 0.6). Due to gravity, the solids are distributed over a small part of the solids inlet channel (stand pipe) cross section only. In the case of aerated inlets (see next) the distribution of solids in the standpipe is more uniform and the solid fraction is lower than the packing limit.

The measured profiles are presented for two cross sections of the riser (Fig. 1): the *YZ* plane is a lengthwise cross section through the middle of the inlet (side inlet positioned at $R = 0.05$ m and $H = 0.5$ m); the *XZ* plane is perpendicular to the *YZ* plane, faces the solids inlet (positioned at $R = 0$ m; $H = 0.5$ m) and goes through the centre of the riser. The origin of the *Z*-axis is at the point where the 0.05 m diameter PVC gas inlet joins the 0.1 m diameter pyrex glass riser (point 21 in Fig. 1, left).

The qualitative interpretation of the vector plots shown in the next paragraph (e.g. Figs. 2 and 3) requires some further explanation. A solids velocity vector is shown at locations allowing a LDA measurement. As such, information on the local data rate is not visible in the vector plots. At locations with a low data rate, i.e., a low solids fraction, the sampling time was increased to retain the accuracy of the velocity measurement. Hence, within the solids fraction window determined by the experimental measurement technique (LDA) (in practice $2.10^{-4} < \varepsilon_s < 0.003$), solids velocity vectors are shown in as well dense as dilute regions of the reactor. The latter allows to gain some insight, although purely qualitatively, in the gas

Table 1
Experimental conditions

	Units	Experimental set-up
Inlet type (see Fig. 1)		Gas: bottom ($\phi = 0.05$ m) Solids: one-side *Y*-type (35° inclined) Aerated/Non-aerated
$S_{\text{gas inlet}}$	(m^2)	0.00196 ($\phi = 0.05$ m) fully developed turbulent profile
$S_{\text{solids inlet}}$	(m^2)	0.005 ($\phi = 0.08$ m), remark*
Superficial gas velocity ($\phi = 0.1$ m)	(m/s)	5.3–6.4–7.4
Gas flow rate Q (in riser)	(m^3/h)	150–180–210
Solids flux G_s (in riser)	($kg/m^2/s$)	0.5–3–4.5
Solids flux G_s^{in} (in inlet channel)	($kg/m^2/s$)	0.79–4.7–7.1
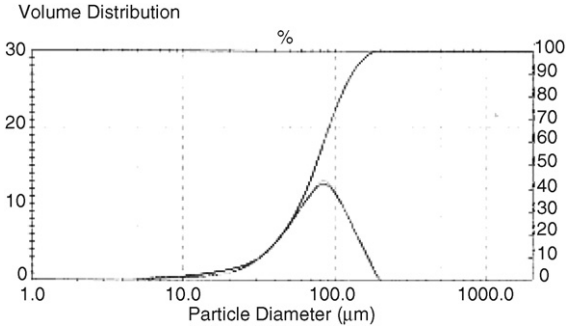		*$\varepsilon_{s,\text{average}}^{\text{in}}$ (in inlet channel when non-aerated) solids enter the riser as a solid jet: with $\phi_{\text{jet,estimated}}$ e.g $G_s = 3\,kg/m^2/s$)= 0.0045 m and $\varepsilon_s^{\text{in}} = \pm 0.6$ instead of $\varepsilon_{s,\text{average}}^{\text{in}}$ uniformly distributed along the whole inlet channel ($\phi = 0.08$ m) Aeration: more uniform distr.< packing limit 0.6
Solids density ρ_s	(kg/m^3)	1550 (FCC), 2650 (silica)
Particle diameter d_p	(μm)	77 (FCC), 260 (silica)
S_{outlet}	(m^2)	0.008 ($\phi = 0.1$ m)
Outlet type (see Fig. 1)		Blinded T (0.34 m extension height)

phase motion as well. To illustrate this, reference is made to Figs. 2(i) and 3(i). Whereas in the dense solids jet the solids velocities are downward, they are upward in the dilute region just below the solids jet (Fig. 2(i))—determined by the upstreaming gas—and in the dilute regions aside of the solids inlet (Fig. 3(i))—indicating preferential upward gas flow aside of the solids inlet. Thus, Figs. 2(i) and 3(i) show that gas is bypassing aside of the dense solids inlet jet. Analogously, Fig. 2(iii) shows some gas bypassing via the side opposite the side solids inlet, resulting in increased axial solids velocities at the side opposite the side solids inlet.

3.1. Bypass effects and hindered gas–solids mixing

3.1.1. Effect of the gas flow rate

Fig. 2 shows the vector plots of the solids velocity ($\overline{v}$) in the *YZ* plane (Fig. 1) for three different gas flow rates (i) 150, (ii) 180 and (iii) 210 m^3/h and a solids flux of 3 $kg/m^2/s$. The experimental observations show that radial gas–solids mixing is hindered near the inlet zone ($z = 0.5$ m, $R = 0.05$ m) and bypassing of the solids by the gas occurs. The bypassing occurs mainly perpendicular to, i.e., around, the *YZ* plane shown (see Fig. 3) but also via the side opposite the solids inlet if the gas flow rate is sufficiently high. The bypassing results in steep velocity gradients and variations in the flow field in the inlet zone of the riser. The presence of a dilute preferential bypass zone (particle sparse region) at the side opposite of the solids inlet becomes more pronounced with increasing gas flow rate. At the lowest gas flow rate of 150 m^3/h (Fig. 2(i)), the solids jet penetrates completely towards the side opposite of the solids inlet and collides with the wall resulting in a high solids concentration zone at the wall opposite the solids inlet. As the gas flow rate increases to 180 m^3/h (Fig. 2(ii)) and the bypassing opposite the solids inlet develops, the solids accumulation opposite the solids inlet decreases. With a further increase of the gas flow rate to 210 m^3/h (Fig. 2(iii)), the bypass zone opposite the solids inlet has grown in width and almost reaches the centre of the riser.

Bypassing results in off-centre maxima in the solids velocity fields. For the higher gas flow rates (180, 210 m^3/h) these maxima remain off-centred beyond 0.54 m height (Fig. 16), while for the lower gas flow rate (150 m^3/h) the velocity profile becomes already more uniform at 0.54 m height with maxima located near the centre of the riser. Although the profiles become more uniform beyond 0.6 m height, it should be remarked that the flow is not fully developed up to 2.35 m height in the riser (see Fig. 16), the measured solids velocities still differing 2–2.5 m/s with the expected fully developed flow values (± 6 m/s (150 m^3/h); ± 7 m/s (180 m^3/h) and ± 8 m/s (210 m^3/h), measured at 6.93 m height in the riser.

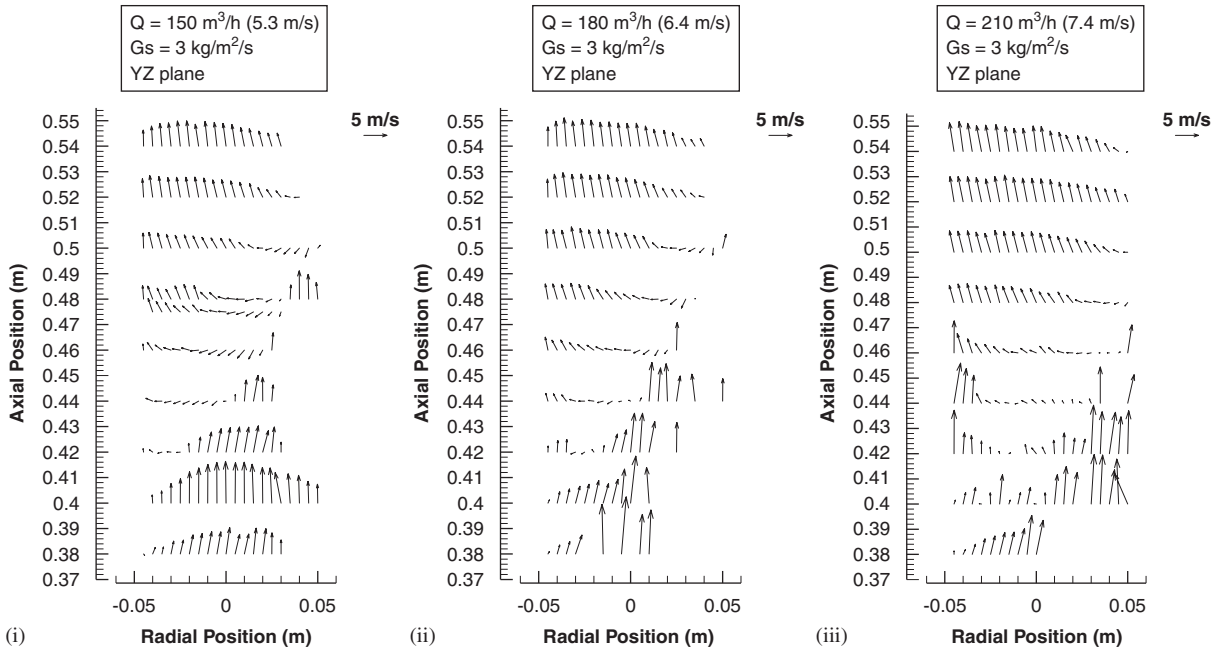

Fig. 2. Solids velocity ($\overline{v}$) in the *YZ* plane for three different gas flow rates (i) 150, (ii) 180, (iii) 210 m^3/h and 3 $kg/m^2/s$ solids flux in the riser. Inlet section between 0.38 and 0.54 m shown. Inlet positioned at $R = 0.05$ m and $H = 0.5$ m. Conditions see Table 1.

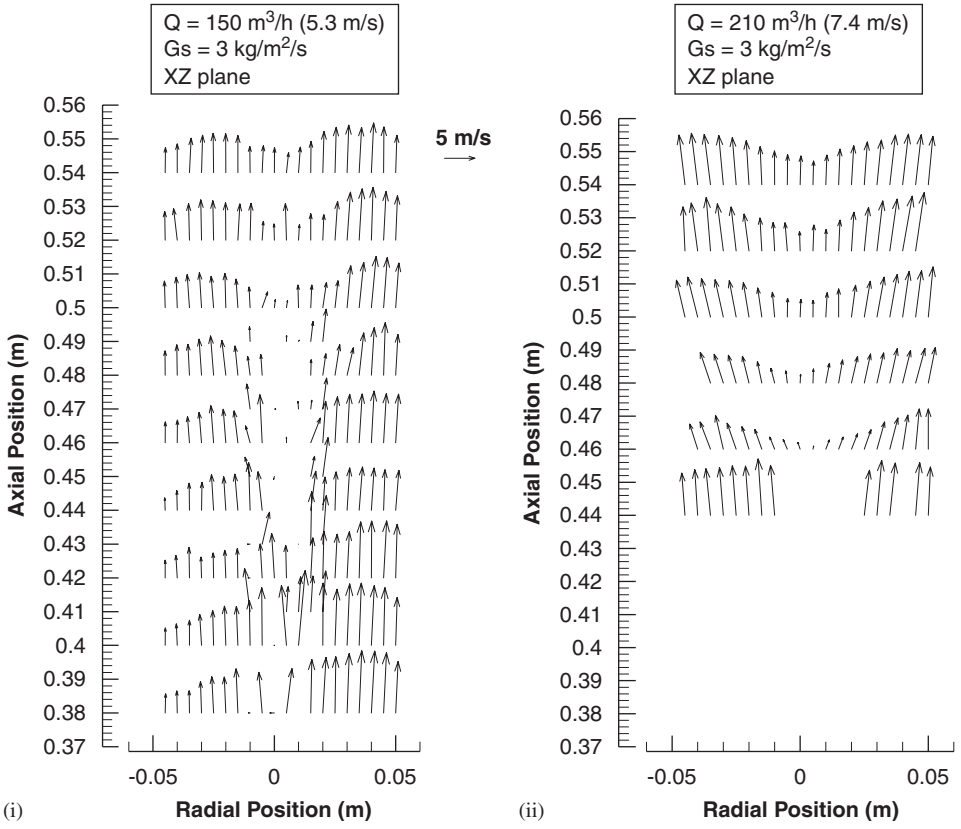

Fig. 3. Solids velocity ($\overline{v}$) in the *XZ* plane facing the solids inlet for two different gas flow rates (i) 150, (ii) 210 m^3/h and 3 $kg/m^2/s$ solids flux in the riser. Inlet section between 0.38 and 0.54 m shown. Inlet positioned at $R = 0$ m and $H = 0.5$ m. Conditions see Table 1.

Fig. 3 shows the vector plots of the solids velocity ($\overline{v}$) in the *XZ* plane (Fig. 1) for gas flow rates of, respectively, (i) 150 and (ii) 210 m^3/h. Although the probe's traversing was perfectly aligned with the inlet geometry and was going through the centre of the riser, it did not seem to be perfectly perpendicular to the solids inlet jet and showed some

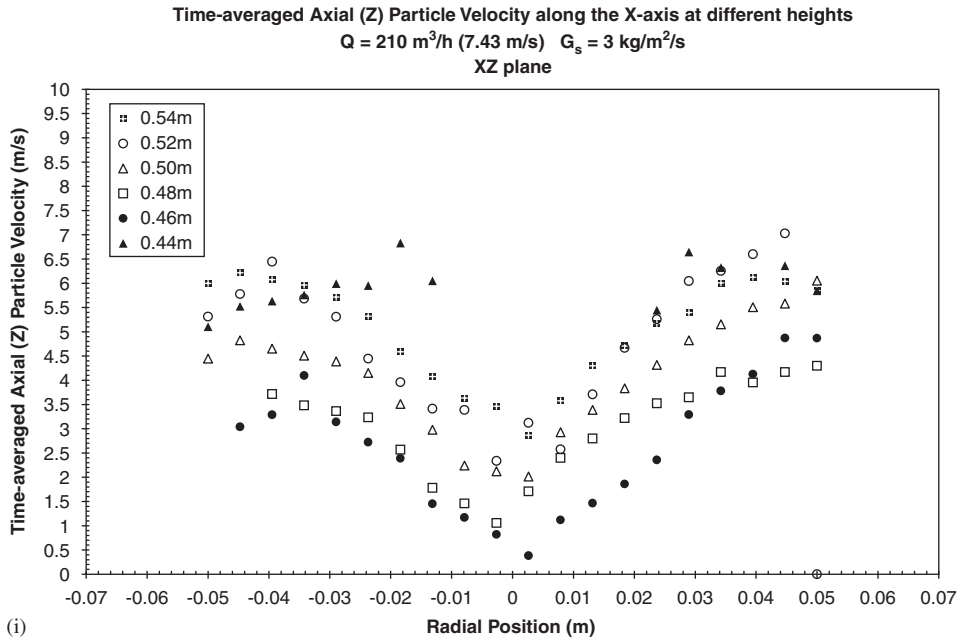

Fig. 4. (i) Time-averaged mean axial (Z) solids velocity, (ii) Time-averaged mean radial (X) solids velocity in the XZ plane along the X-axis for 210 m^3/h gas flow rate and 3 $kg/m^2/s$ solids flux in the riser. Inlet section between 0.44 and 0.54 m shown. Inlet positioned at $R=0$ m and $H=0.5$ m. Conditions see Table 1.

asymmetry. This can be attributed to the small imperfectness of the internal geometry of the glass works which in fact internally makes a small angle with the YZ plane. Additionally, it is further examined whether influences of the gas inlet (90° with YZ plane) and astigmatism effects have any contribution to these asymmetries.

It is clear that bypassing of the solids by the gas is a 3D phenomenon and does not only occur opposite the solids inlet in the YZ plane (Fig. 2), but mainly aside of the solids inlet jet. In Fig. 3(i), the central blank zone corresponds with the downwards flowing solids jet. The high solids concentration in this jet does not allow a measurement with the LDA, due to blocking of the laser beams. Fig. 3(ii) (210 m^3/h) confirms that with higher gas flow rates the jet is entrained more quickly, i.e., at a higher position in the riser (all velocities are positive, no central blank zone). The blank zone at locations below 0.44 m in Fig. 3(ii) is due to the total absence of particles in the bottom region of the riser, confirming an improved solids entrainment by the gas. As an example, Fig. 4 shows the quantitative data of the axial (Z)

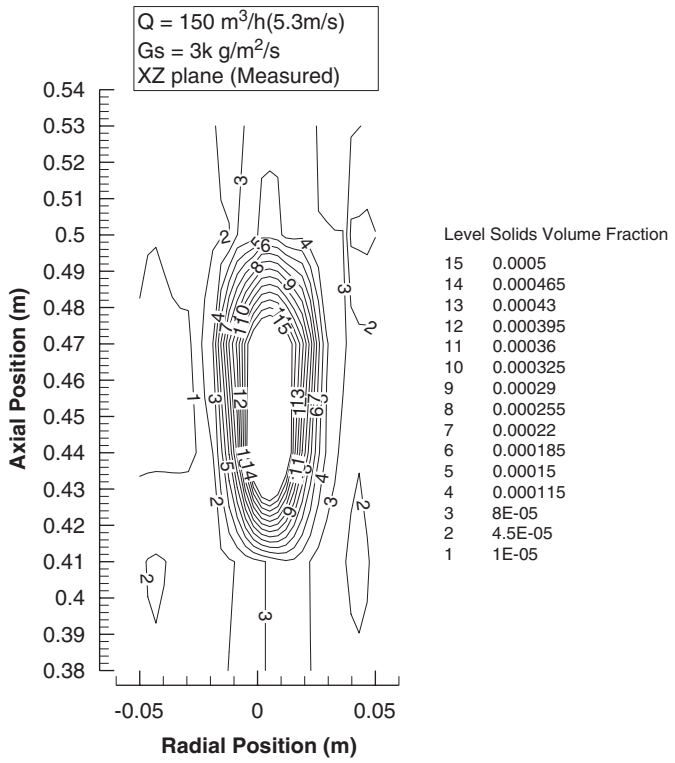

Fig. 5. Time-averaged solids volume fraction in the XZ plane for 150 m^3/h gas flow rate and 3 $kg/m^2/s$ solids flux in the riser. Inlet section between 0.38 and 0.54 m shown. Inlet positioned at $R = 0$ m and $H = 0.5$ m. Conditions see Table 1 (note the values shown are estimates).

and radial (X) mean velocity corresponding to the vector plot in Fig. 3(ii).

With increasing gas flow rate, the radial component (X) of the solids velocity increases, the off-centred maxima of the axial (Z) solids velocities become more pronounced, and the positions of the off-centred maxima shift towards the wall (Figs. 3 and 4). Moreover, the radial (X) component is quite large (up to 1.5 m/s for 210 m^3/h). Finally it should be noted that the profiles in Fig. 3 are asymmetric, especially in Fig. 3(i). It is to be verified whether this can be attributed to the asymmetric 90° side gas inlet (see Fig. 1) or to the imperfectness of the side solids inlet configuration itself (pyrex glass).

Fig. 5 shows an estimate of the solids volume fraction inside and outside the solids jet. It should be mentioned that the accuracy of these measurements is rather low, but Fig. 5 nicely illustrates the origin of bypassing, the upflowing gas being hindered by a dense solids region.

Fig. 6 shows the solids axial (Z) and radial (X) root mean square (RMS) velocities in the XZ plane for, respectively, (i) 150 and (ii) 210 m^3/h gas flow rate. The fluctuating RMS velocity is a measure of the particle velocity fluctuations which play an important role in mixing. Values of the granular temperature can be qualitatively compared with the experimentally obtained RMS particle velocity fluctuations. The highest velocity fluctuations, both axial (Z) and radial (X) occur at the boundaries of the solids jet, in and under the bypass zones where the gradients in the mean solids velocity (Fig. 3) are the most pronounced. The corresponding fluctuating motion intensities are 20–40%. Fig. 6 confirms that increasing the gas flow rate results in increasing axial (Z) and radial (X) fluctuating particle velocities.

A clear anisotropy between the axial (Z) and radial (X) fluctuating particle velocities, by about a factor of 2, is observed, the axial fluctuations being more pronounced (1.5 versus 0.7 m/s). A comparison with values taken from the fully developed zone (anisotropy ratios up to a factor 2–4) reveals that the RMS fluctuating velocity field is developing after a return to isotropy in the inlet zone of the riser. The anisotropy in the velocity fluctuations is inherent in fully developed gas–solid flow and is probably related to the presence of the solid wall of the riser and/or gravity.

3.1.2. Effect of the solids flux

Fig. 7 shows the vector plots of the solids velocity in the YZ plane for three different solids fluxes, respectively, (i) 0.5, (ii) 3 and (iii) 4.5 $kg/m^2/s$ for a gas flow rate of 150 $kg/m^3/h$. A solids jet penetrates towards the side opposite the solids inlet and bypassing occurs mainly aside of the solids jet, i.e., in the XZ plane (e.g. Fig. 3(i)). However, with decreasing solids flux, a tendency for the development of a bypass zone in the YZ plane at the side opposite of the solids inlet is observed.

At higher fluxes (3–4.5 $kg/m^2/s$) solid particles are present in the zone below the solids jet, almost down to the riser bottom, allowing LDA measurements of particle velocities in the regions immediately below the solids jet. In the case of 0.5 $kg/m^2/s$ flux, no solid particles were detected underneath the solids inlet jet.

Fig. 8 shows the influence of the solids flux on the measured axial (Z) and radial (Y) fluctuating velocities in the YZ plane. With increasing solids flux, the axial (Z) fluctuating particle velocities increase, whereas the radial (Y) fluctuating particle velocities hardly change. Hence, anisotropy clearly increases with increasing solids flux. Fluctuating motion intensities rise from 30% to 50% in the part upstream and from 0% to 50% in the part downstream the solids jet. In the solids jet itself fluctuating motion intensities reach 50%.

3.2. The effect of aeration

According to Cheng et al. (1998) the condition and rate of the entering solids affect to a large extent the riser bottom operation, i.e., hold-up, the length of the acceleration zone, mixing and transfer phenomena. Arastoopour (2001a) stated that local aeration in the standpipe resulted in less accumulation in the inlet and in more uniform inlet mixtures into the riser. Therefore, experiments with an aerated side solids inlet are performed. The inlet geometry was modified by connecting a small aeration device (1 m^3/h flow rate) to the standpipe located near point 22 in Fig. 1 (left), which ensured the solids jet to become more uniform near the riser injection point (Fig. 1, right). The aeration device consists of one single metal aeration tap (internal diameter 4 mm, located 0.2 m away from the inlet opening) that is connected to the compressor system (4 barg) by means

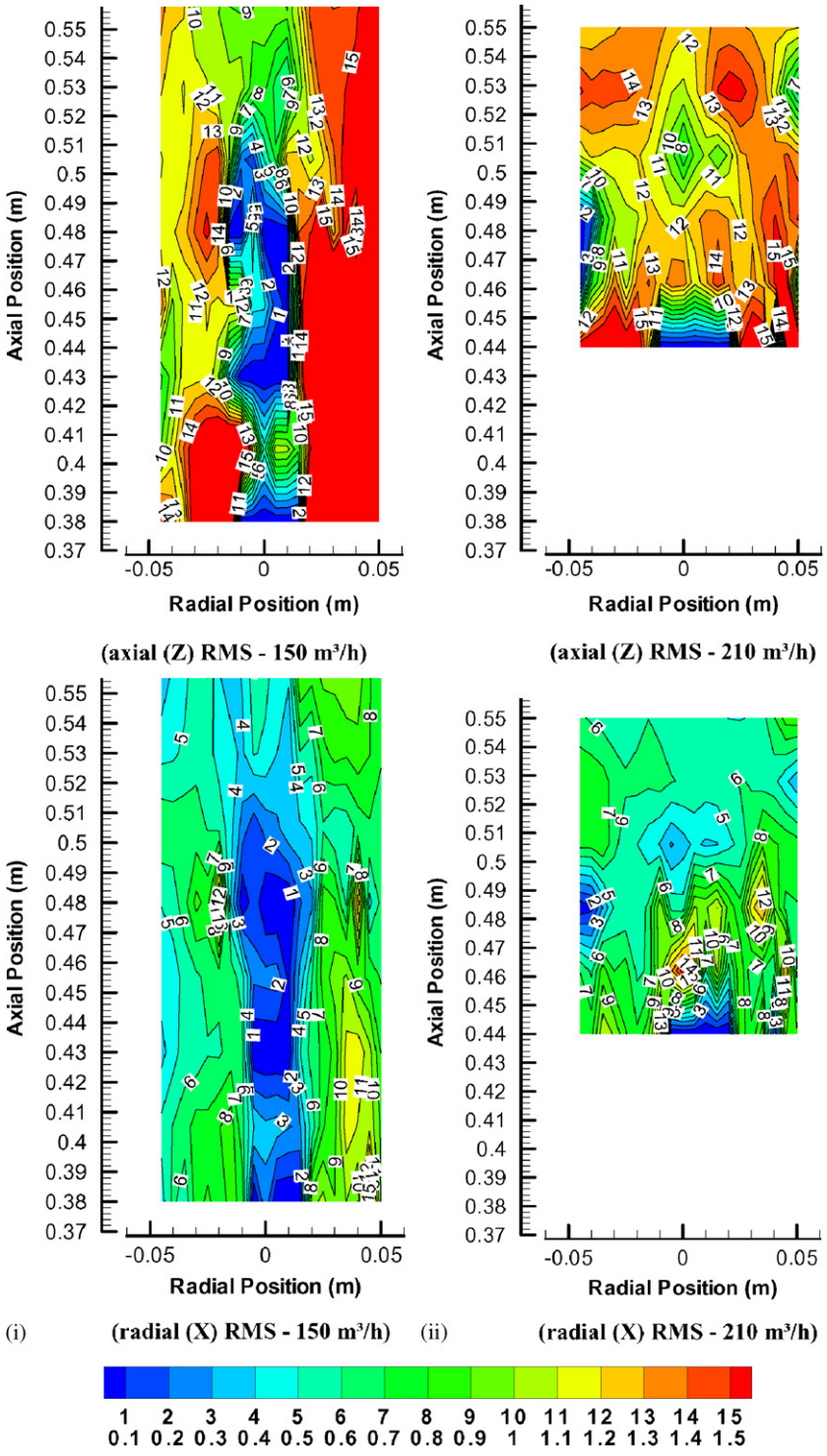

Fig. 6. Solids axial (Z) and radial (X) RMS fluctuating velocity (m/s) in the XZ plane facing the solids inlet for two different gas flow rates (i) 150 and (ii) 210 m^3/h and 3 $kg/m^2/s$ solids flux. Inlet section between 0.37 and 0.55 m shown. Inlet positioned at $R = 0$ m and $H = 0.5$ m. Conditions see Table 1.

of a flexible wire. A pressure regulator allows manipulating the inlet pressure from 4 to 0.6 barg, corresponding with changes in air flow rates (indicated by a rotameter) from 0 to 5 m^3/h. At the end of the aeration tap, a gas distributor, consisting of a 0.01 m long sintered metal piece, was welded. The gas distributor reduces the available air flow rate to about 1 m^3/h.

Fig. 9 shows the solids velocity ($\overline{v}$) in the YZ plane obtained with the aerated side solids inlet for, respectively, (i) 150 and (ii) 210 m^3/h gas flow rate and a solids flux of 0.5 $kg/m^2/s$ in the riser. Bypass of the solids by the gas results in the formation of velocity profiles with off-centre maxima. In contrast with the non-aerated inlet (Fig. 7(i)), gas mainly bypasses via

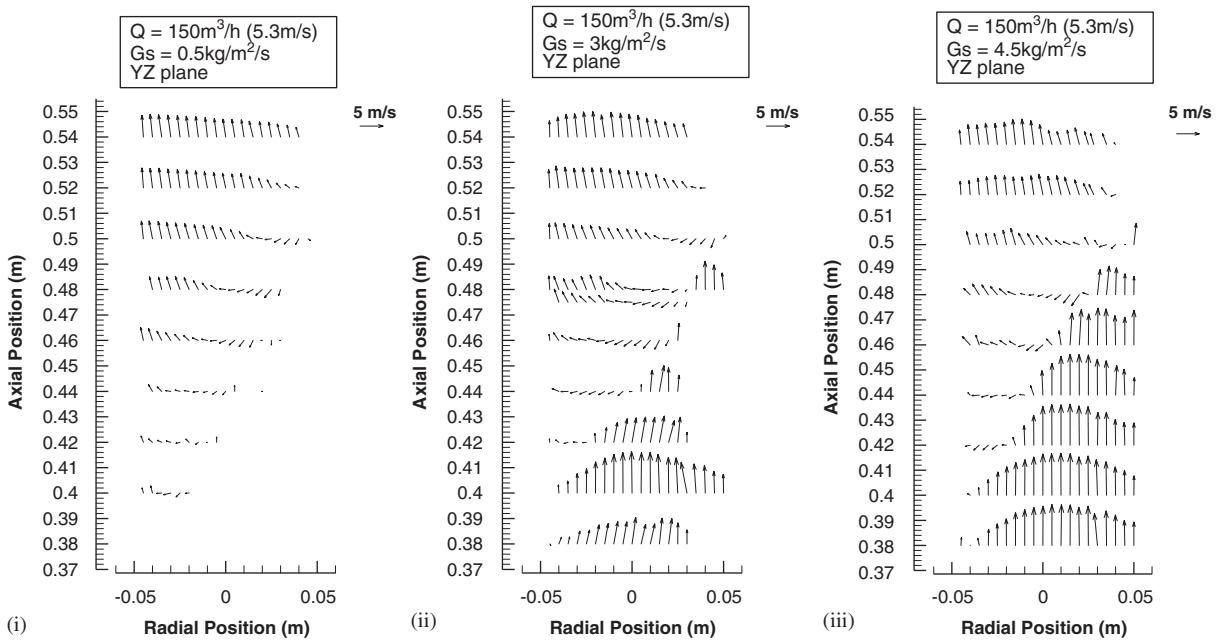

Fig. 7. Solids velocity ($\overline{v}$) in the *YZ* plane for three different solids fluxes (i) 0.5, (ii) 3 and (iii) 4.5 kg/m^2/s and gas flow rate 150 m^3/h in the riser inlet. Inlet section between 0.38 and 0.54 m shown. Inlet positioned at $R = 0.05$ m and $H = 0.5$ m. Conditions see Table 1.

the side opposite the solids inlet (*YZ* plane) (Fig. 9) even at a gas flow rate of 150 m^3/h. The dense reactor zone bypassed by the gas reduces significantly in volume when aerating the side solids inlet. For a gas flow of 210 m^3/h the width of the bypass zone remains about the same as for 150 m^3/h, but the solids fall to 0.46 m height while for a gas flow of 150 m^3/h they fall somewhat deeper to 0.44 m height. The blank zone at lower locations in Fig. 9 illustrates the total absence of particles in the bottom region of the riser in the case of aerated inlets. The measured solids velocity profiles are found to be very sensitive to aeration of the solids inlet channel, showing that the inlet design can significantly change the overall performance of the riser reactor. Due to predilution in the solids jet, aeration improves the solids entrainment to a larger extent than increasing the gas flow rate (Fig. 2) or lowering the solids flux (Fig. 7).

A quantitative comparison between non-aerated and aerated inlets of the time-averaged mean axial (Z) velocity at 0.56 m height in the *YZ*-plane (gas flow rate 150 m^3/h, solids flux 0.5 kg/m^2/s) is presented in Fig. 10. Fig. 10 reveals that in case of aeration the acceleration zone is indeed firmly reduced (solid velocities up to 4.5 versus 3.5 m/s).

In general, as with the non-aerated solids inlet, the axial (Z) and radial (Y) fluctuating RMS velocities in the *YZ* plane (not shown here) increase with increasing gradients in the mean axial (Z) and radial (Y) velocities. Increasing the gas flow rate results in an increase of the axial (Z) RMS particle velocities in the *YZ* plane, but in a decrease of the radial (Y) RMS velocities. The gas flow that bypasses the solid jet in the *YZ* plane in the case of aerated inlets has a stabilizing effect on the radial (Y) velocity fluctuations. A maximum in both the axial (Z) and radial (Y) velocity fluctuations is observed in front of the inlet opening in the region where upflow and downflow, induced by the inlet effect, encounter. Radial (Y) velocity fluctuations are damped near the riser side wall.

Compared with the non-aerated profiles, aerated inlets give way to more uniform axial (Z) and radial (Y) fluctuations in the whole inlet zone. Secondly, only a slight anisotropy between the axial (Z) and radial (Y) fluctuating particle velocities has been observed, meaning that the aerated inlets give way to more isotropic fluctuations near the inlet jet. Relatively speaking, the intensity of the fluctuating motion is about 20–25%, which is lower compared with the non-aerated inlets.

Fig. 11 shows the solids velocity ($\overline{v}$) in the *XZ* plane with an aerated side solids inlet for a solids flux of 0.5 kg/m^2/s and gas flow rates of,respectively,(i) 150 and (ii) 210 m^3/h. Bypass in the *XZ* plane still occurs,but is less pronounced in comparison with the non-aerated side solids inlet (Fig. 3). It should be noted that the measurements from Fig. 11 are taken at 0.5 kg/m^2/s flux. Measurements at 0.5 kg/m^2/s (without aeration) and at 3 kg/m^2/s (with aeration) are not included. The influence of aeration is by far the most important phenomenon leading to an improved gas–solids mixing,rather than lowering the solids flux from 3 to 0.5 kg/m^2/s. In contrast with Fig. 3 no downward flowing particles are detected in the *XZ* plane (blank zone in Fig. 3) and the jet appears to be more dilute making LDA measurements possible because there is no blocking of the laser beams. Moreover a blank zone at locations lower than 0.44 m height illustrates the total absence of particles in the bottom region of the riser and confirms that the jet is entrained much easier. As seen from Fig. 11 higher gas flow rates result in higher off-centred maxima in the solids velocity profile. Fig. 11 shows that the radial component (X) of the solids velocity is also quite large (up to 1.5 m/s). This indicates an

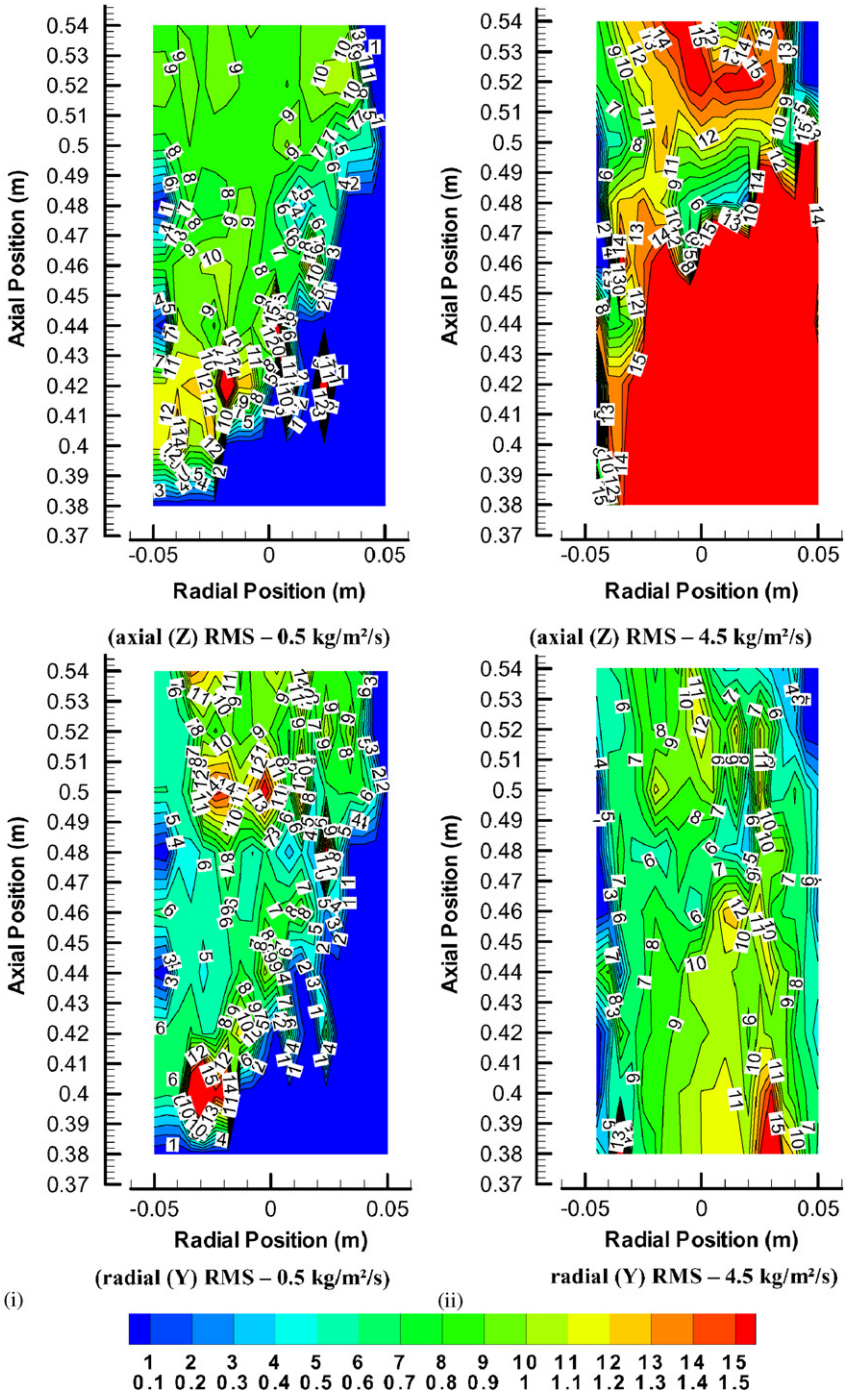

Fig. 8. Solids axial (Z) and radial (Y) fluctuating RMS velocity (m/s) in the YZ plane for two different solid fluxes (i) 0.5 kg/m^2/s and (ii) 4.5 kg/m^2/s. Inlet section between 0.37 and 0.55 m shown. Inlet positioned at $R = 0.05$ m and $H = 0.5$ m. Conditions see Table 1.

overall good radial mixing of the solids. With increasing gas flow rate,the radial component (X) of the solids velocity slightly increases and the off-centred maxima shifts towards the wall. It should be remarked that the radial (X) velocity component induced by the side solids inlet is only slightly affected by the gas flow rate and its dependence on the gas flow rate is less pronounced than in the case of the non-aerated inlet (Figs. 3 and 4). The radialupward dissipation results in a conical shape of the zone in which particles are detected (Fig. 11). As a result the angle of the conus decreases with increasing axial velocity—that is gas flow rate. Finally, it should be noted that in comparison with the non-aerated profiles from Fig. 3, the profiles in Fig. 11 are more symmetric as compared to the profiles obtained with the non-aerated inlet and illustrate the presence of a more uniform and more dilute solids jet compared to a non-aerated solids inlet (Figs. 3 and 5), resulting in broader bypass

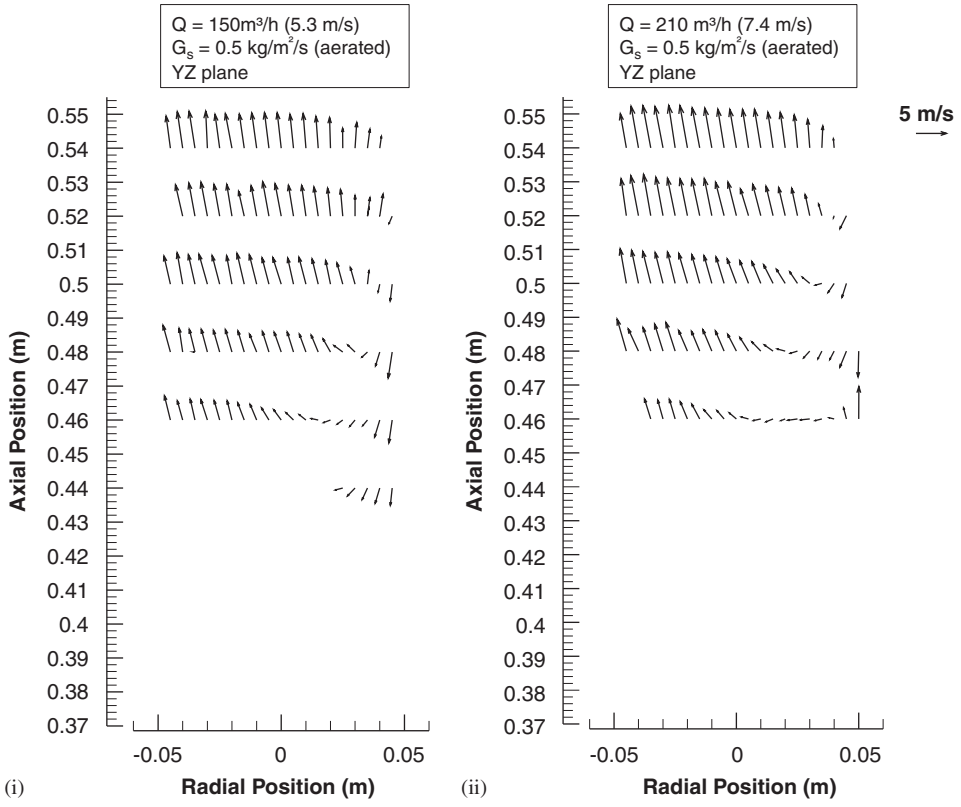

Fig. 9. Solids velocity ($\overline{v}$) in the *YZ* plane for an aerated (homogenized) inlet for gas flow rates (i) 150 m^3/h and (ii) 210 m^3/h and 0.5 $kg/m^2/s$ solids flux in the riser. Inlet section between 0.38 and 0.54 m shown. Inlet positioned at $R = 0.05$ m and $H = 0.5$ m. Conditions see Table 1.

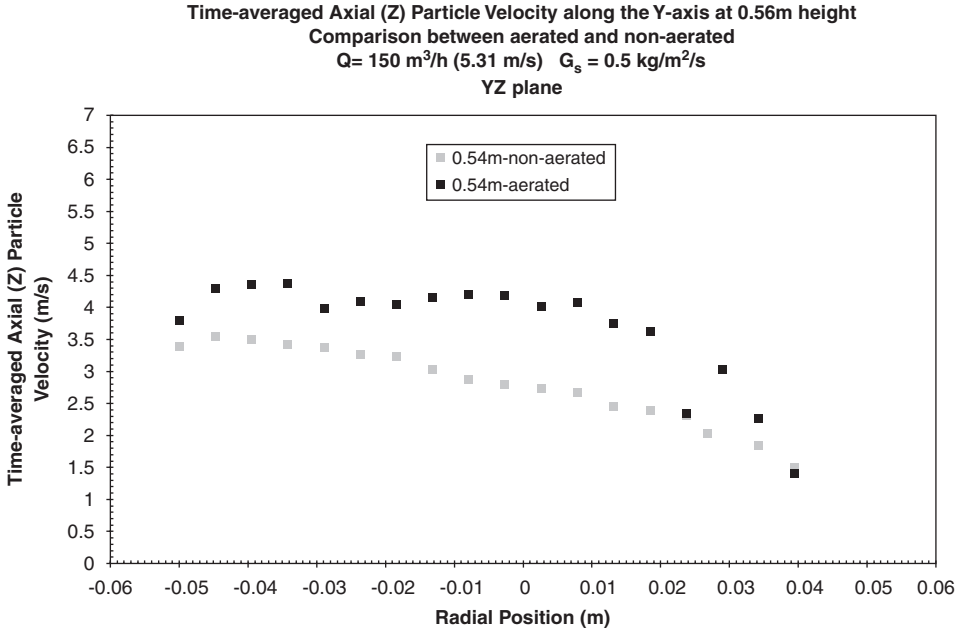

Fig. 10. Time-averaged mean axial (Z) solids velocity in the *YZ* plane along the *Y*-axis at 0.56 m height for 150 m^3/h gas flow rate (0.5 $kg/m^2/s$ solids flux). Quantitative comparison between aerated and non-aerated inlet. Inlet positioned at $R = 0.05$ m and $H = 0.5$ m. Conditions see Table 1.

zones opposite the solids inlet and in improved gas–solids mixing. Additional dilution of the solid jet by increases in gas flow rate (150–210 m^3/h) is occurring.

Fig. 12 shows for an aerated solids inlet the solids axial (Z) and radial (X) RMS velocities in the *XZ* plane for (i) 150 and (ii) 210 m^3/h gas flow rate. The highest velocity fluctuations,

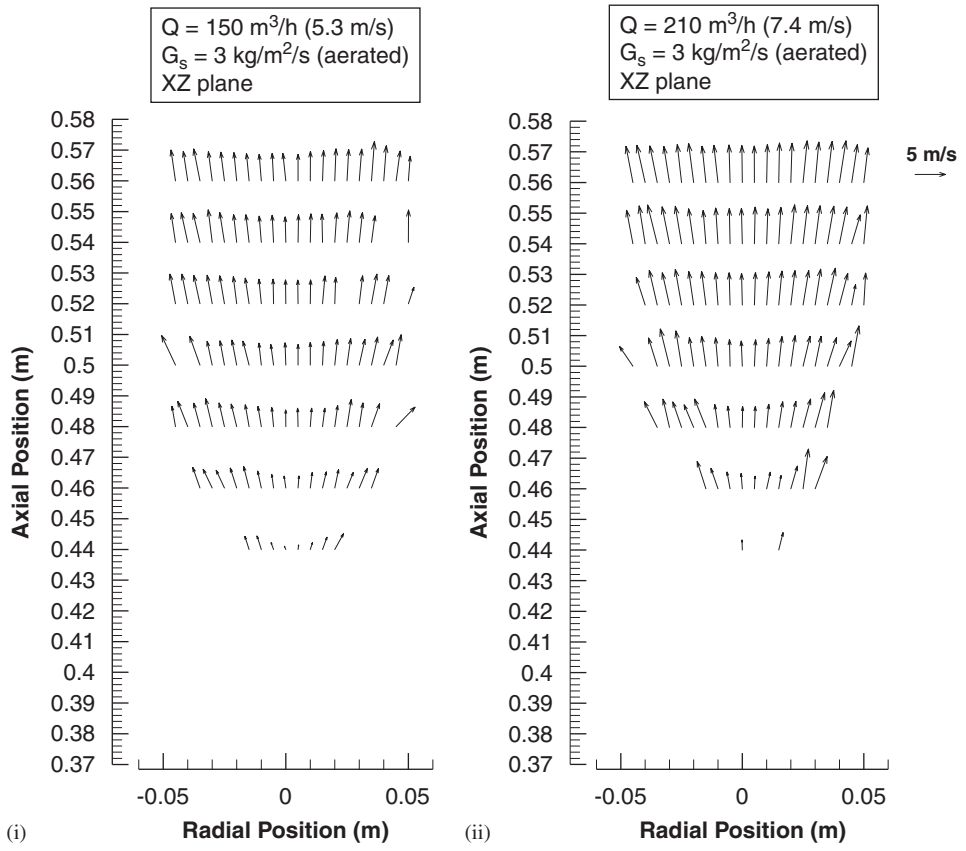

Fig. 11. Solids velocity ($\overline{v}$) in the *XZ* plane for an aerated inlet for gas flow rates (i) 150 m^3/h and (ii) 210 m^3/h and 0.5 $kg/m^2/s$ solids flux in the riser. Inlet section between 0.38 and 0.56 m shown. Inlet positioned at $R = 0$ m and $H = 0.5$ m. Conditions see Table 1.

both axial (Z) and radial (X), occur at the boundaries of the solids jets, especially aside the bypass zones where the gradients in the mean solids velocity (Fig. 11) are the most pronounced. The corresponding fluctuating motion intensities are 20%, which is lower than with the non-aerated inlet. Increasing the gas flow rate results in increasing axial (Z) RMS fluctuating particle velocities and in decreasing (damped) radial (X) RMS fluctuating particle velocities. In the case of a high flow rate (210 m^3/h), isotropy in the axial (Z) and radial (X) fluctuating particle velocities, is observed. For the lowest flow rate of 150 m^3/h, the radial fluctuations become more pronounced than the axial (Z) fluctuations (1.5 m/s versus 0.8 m/s).

3.3. Influence of the particle type

In addition to FCC catalyst (Geldart A type), measurements using silica particles with a mean volume averaged diameter of 260 μm and a solids density 2650 kg/m^3 (Geldart B type), and particle size distribution given by Van engelandt et al. (2004), are presented. This allows quantification of the influence of the particle size and density on the observed inlet flow profiles. Experiments show that in general the same abrupt inlet phenomena occur as detected with FCC particles (Figs. 2 and 3), i.e., hindered radial gas–solids mixing and bypassing of the solids jet aside and opposite the solids inlet.

To a larger extent than changing the overall flow patterns, the type of particles greatly influences the length of the acceleration zone downstream the inlet. A quantitative comparison of both types of particles is shown in Fig. 13 for the non-aerated solids inlet. The axial (Z) solids velocities in the *YZ* plane at a height of 0.52 m (Fig. 13) show much lower values for the silica particles than for the FCC particles (0.5–1 versus 1–3.5 m/s, negative solid jet not taken into account). Fully developed flow profiles (average velocities of 3–4 m/s for silica and 5–6 m/s for FCC, see Figs. 15 and 16 and Van engelandt et al., 2004) indicate that at 0.52 m height the FCC particles have reached already 60% of the fully developed velocity value while for silica this is only 20–25%. This shows that in the case of silica particles, the acceleration zone is firmly extended (approximately by factor of 3). The same conclusions can be drawn from the velocities in the *XZ* plane at 0.46 m height (not shown): values 0.5–2 m/s in the bypass zones for silica versus 2.5–6 m/s for FCC particles (negative solid jet not taken into account). It should be noted that profiles in the *XZ*-plane with silica did allow measurements in the downward flowing part of the solids jet. This is explained by the lower number of bigger silica particles that are present in a solids jet of constant flux 3 $kg/m^2/s$.

Finally, in comparison with Fig. 10 (non-aerated solids inlet), Fig. 13 shows that higher solids fluxes (3 $kg/m^2/s$ versus 0.5 $kg/m^2/s$) give way to less (radially) uniform profiles.

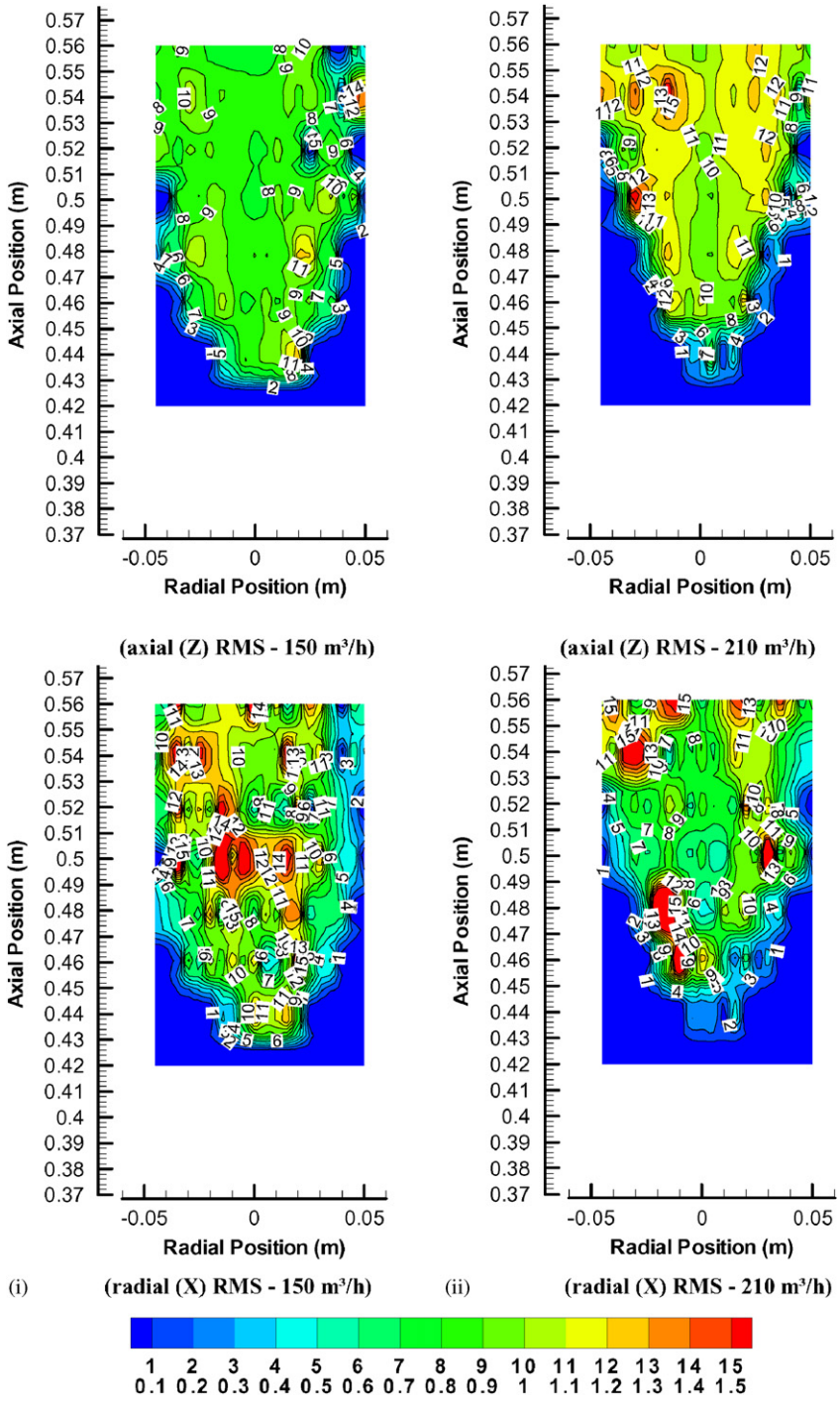

Fig. 12. Solids axial (Z) and radial (X) fluctuating RMS velocity (m/s) in the XZ plane for an aerated inlet for two different gas flow rates (i) 150 and (ii) 210 m^3/h and 0.5 $kg/m^2/s$ solids flux. Inlet section between 0.37 and 0.55 m shown. Inlet positioned at $R = 0.05$ m and $H = 0.5$ m. Conditions see Table 1.

Axial (Z) and radial (Y or X) RMS fluctuating particle velocities in the YZ and XZ planes have also been compared for FCC and silica particles (figure not shown). Larger and heavier particles (silica) clearly result in lower axial and radial RMS fluctuating velocities, both in the YZ-plane as well as in the XZ-plane. It shows that inertial effects can significantly influence the length of the bottom mixing zone in the riser. Note that in the solid jet itself, RMS fluctuating velocities are equal for both types of particles.

3.4. Vortex formation

In the immediate vicinity of the side solids inlet, the gas flow and the particle flow are still weakly coupled. The gas

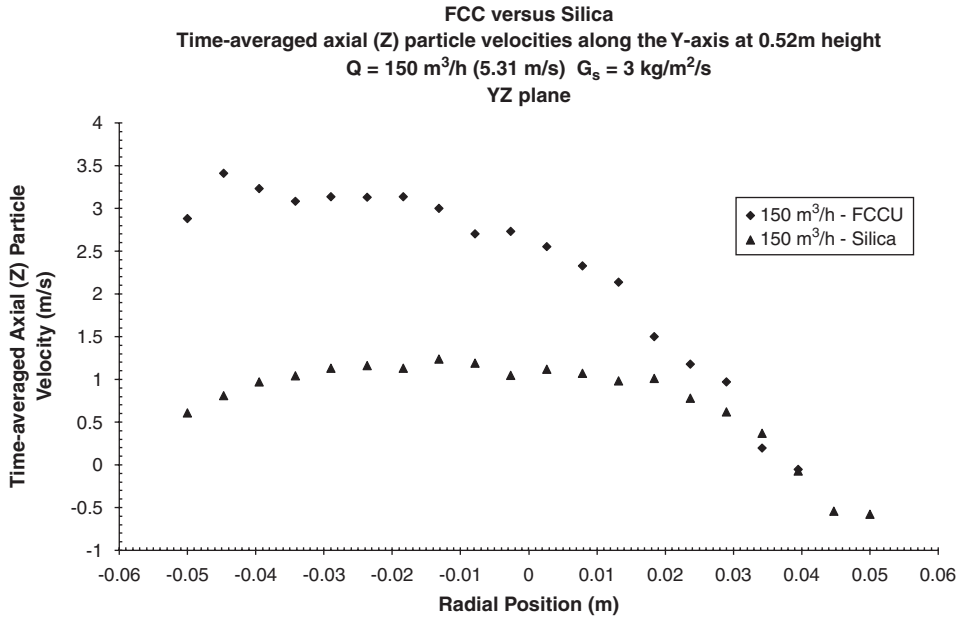

Fig. 13. Time-averaged mean axial (Z) solids velocity in the YZ plane along the Y-axis at 0.52 m height for 150 m^3/h gas flow rate and 3 $kg/m^2/s$ solids flux in the riser. Comparison between FCC and silica particles. Inlet positioned at $R = 0.05$ m and $H = 0.5$ m. Non-aerated case. Conditions see Table 1.

stream (from the riser bottom) flows upwards, while the solids phase (from the standpipe) is forced to make a 155° inclined turn into the riser. Inertia causes the inlet solids jet to (initially) move straight into the riser bottom (that is 35 ° inclined with Z-axis). The solids velocities ($\overline{v}$) in the YZ plane through the centre of the inlet are shown for a gas flow rate of 150 m^3/h in Fig. 14. A macro-scale vortex is formed by the 35° Y-inlet configuration, inducing recirculation. The vortex has a 3D nature, but mainly recirculates some flow (gas and also solids) back to about 0.05 m into the upper dilute part of the standpipe. Visual observations and the measured data rate indicate an increased solids hold-up in the eye of the (dilute) recirculation vortex. Increasing the gas flow rate increases the vorticity magnitude of the macro-scale vortex in the standpipe. The vorticity is a measure of the rotation of a fluid element as it moves in the flow field, and is defined as the curl of the velocity vector ($\nabla \times \overline{v}$).

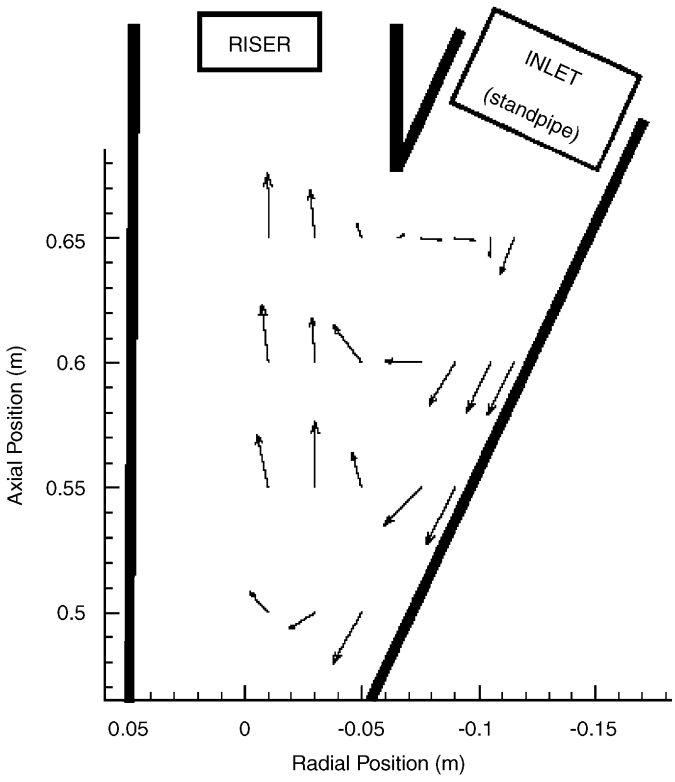

Fig. 14. Solids velocity ($\overline{v}$) in the YZ plane for gas flow rate 150 m^3/h and 3 $kg/m^2/s$ solids flux in the riser. Vortex formation phenomena near the inlet opening. Inlet section between 0.5 and 0.65 m shown. Inlet positioned at $R = -0.05$ m and $H = 0.5$ m. Non-aerated case. Conditions see Table 1.

3.5. Reflection phenomena

It was shown in the previous paragraph, that in the case of a gas flow of 210 m^3/h and a solids flux of 3 $kg/m^2/s$ (Fig. 2(iii)) a full entrainment of the particles jet resulted in the appearance of a bypass zone opposite the side of the solids inlet. Also a widening of the bypass zones in the XZ plane was seen at higher gas velocities (Fig. 3). Fig. 15 now focuses on effects more downstream in the riser (section 0.45–8 m) and shows in particular the vector plots of the solids velocity ($\overline{v}$) in the YZ plane for a gas flow of 210 m^3/h and a solids flux of 3 $kg/m^2/s$ FCC particles (i) in the inlet section of the riser at 0.45–1 m height; (ii) in the developing zone at 1.2–2.5 m height and (iii) in the fully developed zone at 4–8 m height (conditions see Table 1). It should be noted that data in Fig. 15 reach as high as 8 m. Outlet effects induced by an L-outlet and T-outlets with different extension heights and outlet surface areas are studied experimentally and computationally for superficial gas

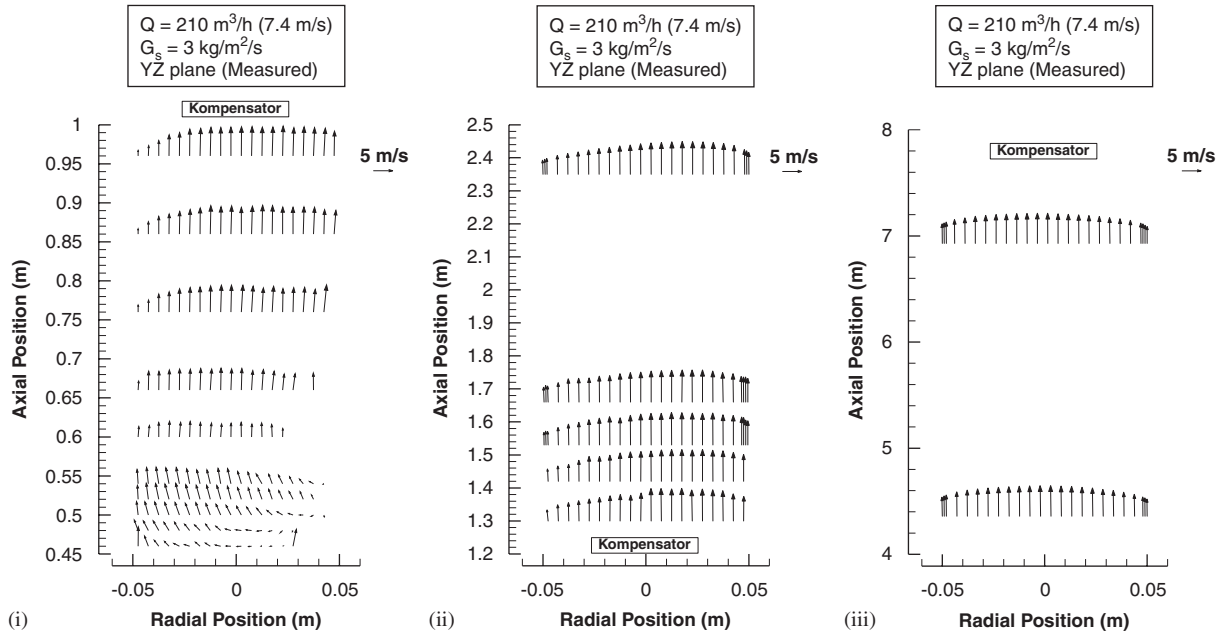

Fig. 15. Reflection phenomena: solids velocity ($\overline{v}$) in the *YZ* plane for 210 m^3/h gas flow rate and 3 $kg/m^2/s$ solids flux in the riser (i) in the inlet section of the riser 0.45–1 m height (ii) in the developing zone 1.2–2.5 m height (iii) in the fully developed zone 4–8 m height. Inlet positioned at $R = 0.05$ m and $H = 0.5$ m. Non-aerated case. Conditions see Table 1.

velocities of 2.65–7.43 m/s and a solids flux of 3.0 $kg/m^2/s$. A T-outlet configuration induces recirculation by vortex formation in the extension part of the riser above the outlet, resulting in steep velocity gradients and off-centre maxima in the velocity field and recirculates the flow along the wall opposite the outlet, inducing reflux down to about 0.1 m upstream of the outlet. In the small diameter riser, the outlet effects can therefore be completely decoupled from the inlet effects (as far as 8 m height). Fig. 15 shows a downstream shift in the location of the maximum solids velocity from the side opposite the solids inlet to the side of the solids inlet, before becoming uniform at axial positions above 4 m. This effect is referred to as "reflection phenomenon" and it results from the tendency of the gas to preferentially follow the path of the least resistance.

Measurements with silica particles in the same set-up at the same conditions (gas velocities 5.31–7.31 m/s and solids fluxes up to 6 $kg/m^2/s$) and using the same inlet geometry were presented at the Fluidization XI conference in Italy (Van engelandt et al., 2004). The results showed a clear swirling motion of particles over the entire riser height. This has been related to combined gas and solid phase inlet effects. It has been visually observed that the same swirling motion, at least in the bottom of the riser, is present when using FCC particles. When particles collide with the wall opposite the solid inlet, solids accumulation contributes to gas bypass effects inducing gas swirl. No further examination however of these effects has been done so far. It is to be verified whether deficiencies of the glass works and gas inlet effects (90° with *YZ* plane) have any significant contribution to these swirl effects. However, the observed reflection phenomenon can be related to the 3D swirling flow.

Sun and Gidaspow (1999) detected a similar bouncing motion of particles in a 2D simulation of the Fluidization VIII Benchmark test (Knowlton et al., 1995) and referred to it as snake-like motion. They also mentioned the sensitivity of this phenomenon towards the inlet geometry (symmetric inlet, side inlet, flat inlet, central inlet, calculating the inlet conditions by taking into account the whole riser loop). In their simulation of the Benchmark test, clusters of solids slowly move downwards and produced a snake-like motion: the gas preferentially flows through the particle sparse regions bypassing the high concentration zones in the riser.

Arastoopour (2001b) investigated similar effects by simulating the Benchmark test of Knowlton et al. (1995) in 3D with a side inlet configuration. It was shown in their results that big clusters descended near the wall opposite the solids inlet and forced the gas to move in different radial positions, resulting in asymmetric solids mass flux profiles. The origin of asymmetric flux profiles was attributed to the combination of inlet and outlet effects.

Fig. 15 clearly shows a reflecting motion observed in the cold-flow LPT riser at 210 m^3/h and 3 $kg/m^2/s$. The dense inlet jet stream is located on the right-hand side at the position of the inlet $R = 0.05$ m and $H = 0.5$ m with $\varepsilon_s = \pm 0.6$. It was shown in Fig. 2(iii) that bypassing occurred on the left-hand side near the inlet zone 0.38–0.54 m and so a particle sparse region is to be expected at the left-hand side of the zone 0.38–0.54 m. At higher positions 0.54–0.85 m near the upper left-hand side, immediately above the side inlet, a high particle concentration region is formed, since the inlet particle jet stream is colliding with the wall opposite the riser inlet (see direction of vectors in the vector plots in Fig. 15). The dense zone at 0.85–2.5 m corresponds with a particle sparse region on the upper right side

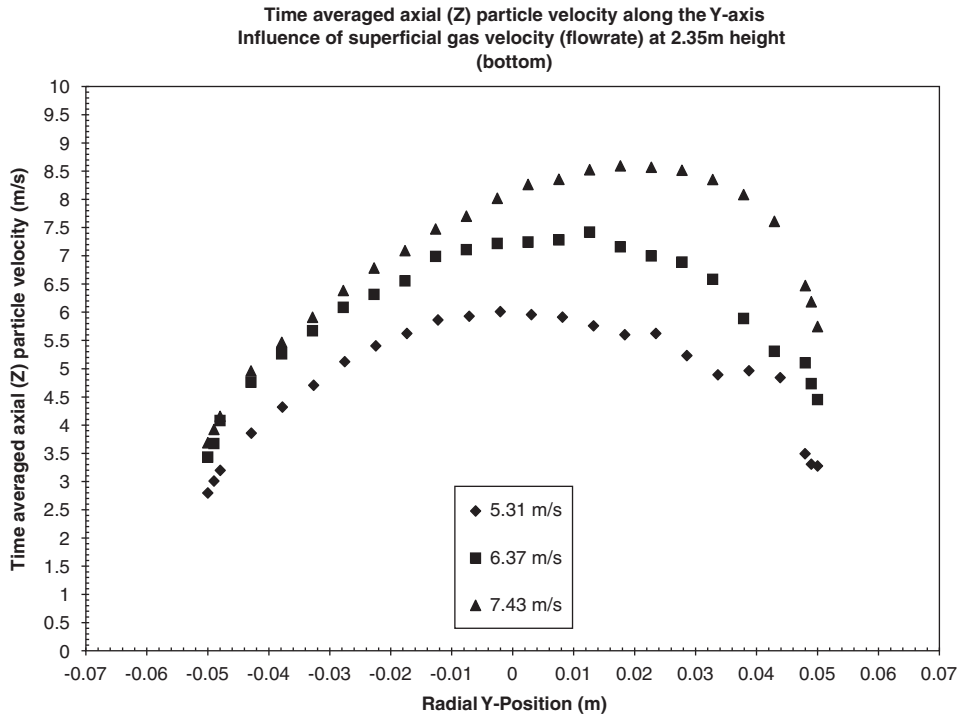

Fig. 16. Axial (Z) solids velocity in the YZ plane along the Y-axis for 150, 180 and 210 m^3/h gas flow rate and 3 $kg/m^2/s$ solids flux in the riser at $H = 2.35$ m. Inlet positioned at $R = 0.05$ m and $H = 0.5$ m. Non-aerated case. Conditions see Table 1. Near solids inlet behaviour: see Fig. 3.

illustrated by the blank zone in Fig. 15(i) in which no particles were measured at all.

It should be noted that comparing with the simulation results of a 0.2 m diameter riser by Arastoopour (2001b), the experimental results in the cold-flow riser show quicker dissipation of the reflection phenomenon: at a height of 4 m the solids velocity distribution becomes radially uniform and an influence of the outlet (blinded T) is hardly observed. Arastoopour (2001b) observed asymmetries in the YZ and XZ plane over the whole riser height. This is attributed to the considerably higher solids fluxes (489 $kg/m^2/s$ in his calculations versus 3 $kg/m^2/s$ in these experiments) and to the larger riser diameter (0.2 versus 0.1 m). The poor radial mixing in large-diameter risers compared to small-diameter risers can be attributed to the reduced impact of the viscous terms.

With an aerated side solids inlet, reflection phenomena are not detected. Aerated inlets result in less dense concentration profiles and more uniform velocity profiles at lower heights (0.6 m, Figs. 9 and 11). Fig. 16 focuses on 2.35 m height in the riser and illustrates the influence of the superficial gas velocity on the time-averaged axial (Z) particles velocities along the Y-axis in the YZ plane. It can be seen that with increasing gas flow rate, the asymmetry in the axial velocity profile and, hence, the reflection phenomenon becomes more pronounced. The location of the reflection point shifts to lower heights at lower gas flow rates. This corresponds with the relocation of the dense zone opposite the riser inlet: at lower gas velocities, the particle jet stream collides with the wall opposite of side solids inlet at lower positions in the riser and consequently the bypassing of this dense zone (so maximum particle velocity at the side $0 < R < 0.05$ m) starts earlier (at lower heights, Figs. 2, 15 and 16).

3.6. Dissipation of non-uniformities

The experimental results for the 0.1 m diameter cold-flow riser, illustrate that in small diameter risers radial mixing quickly dissipates bypassing effects and the profiles become uniform 0.6 m downstream in the riser (Figs. 2, 3, 7, 9, and 11). Dissipation is fast, especially in the case of aerated inlets and small particles (Geldart A type). The latter is in accordance with simulations for small diameter risers (De Wilde et al., 2003b, 2005), but in contrast with what is seen in simulations of large diameter industrial scale risers (De Wilde et al., 2003b, 2005). The bypass effects in small diameter, low flux risers are quickly dissipated by the viscous forces. The impact of the former is less in large diameter risers.

With FCC particles, the experimental observations in the cold-flow riser show that the acceleration zone for the lower gas flow rates 150–180 m^3/h (3 $kg/m^2/s$ solids flux) is maximum 2.35 m long for non-aerated inlets (Fig. 16) and shorter for aerated inlets. For the case of a non-aerated solids inlet and the higher gas flow rate of 210 m^3/h, reflection phenomena extend the acceleration zone beyond 2.35 m height. Reflection phenomena are not detected with aerated inlets. In all cases, the FCC solids velocity profiles become radially

uniform below 4 m pilot riser height. In case silica particles are used, the acceleration zone is further extended reaching 6 m height.

4. Conclusions

The influence of a side solids inlet on the flow pattern in a dilute phase riser is investigated experimentally in a cold-flow pilot riser. Accurate quantitative 3D-LDA data are provided. Experiments show that the condition, the type (Geldart A versus B) and the rate of solids feeding affect the riser bottom operation and the gas–solids mixing to a large extent. Larger particles extend the length of the acceleration zone. Gas–solids mixing in the riser is hindered by an abrupt entry of the solids due to bypassing of dense solids regions by the gas. Higher gas flow rates and lower solids fluxes allow bypassing to occur in the plane of the solids inlet via the side opposite the solids inlet. As a result, bypassing in the plane facing the solids inlet i.e., aside of the solids inlet, is reduced. In the immediate vicinity of these bypass zones, RMS fluctuating velocities (axial and radial) increase. Using a more uniform aerated side solids inlet, the solids are entrained faster, resulting in broader bypass zones opposite the solids inlet and in improved gas–solids mixing with more uniform fluctuating motions. A non-aerated Y-inlet configuration induces a small reflux into the upper dilute part of the standpipe.

In small diameter risers, radial mixing quickly dissipates the non-uniformities introduced by a side solids inlet. However, reflection phenomena occur in the bottom zone of the riser in the case of non-aerated inlet conditions, extending the length of the non-uniform reactor zone. The experimental data describe well the solids acceleration behavior and can be used to validate gas–solids flow models via 3D simulations.

Acknowledgements

The authors acknowledge graduating student F. Vercoutter for his major contributions to the experimental work. The “Instituut voor de aanmoediging van Innovatie door Wetenschap en Technologie in Vlaanderen (IWT-Vlaanderen)” is acknowledged for the financial support under contract IWT/OZM/020059. The “Bijzonder Onderzoeksfonds van de Universiteit Gent” and the IAP programme of the Belgian Federal Science Policy are acknowledged for the financial support of the FCC-research. EXXONMOBIL (Esso refinery Antwerp) is greatly acknowledged for supplying the FCC catalyst (Engelhard corp.).

References

Agrawal, K., Loezos, P.N., Syamlal, M., Sundaresan, S., 2001. The role of meso-scale structures in rapid gas–solid flows. Journal of Fluid Mechanics 445, 151–185.

Arastoopour, H., 2001a. Fluent news Winter 2001 Courtesy of Hamid Arastoopour. Department of Chemical and Environmental Engineering, Illinois Institute of Technology, USA.

Arastoopour, H., 2001b. Numerical simulation and experimental analysis of gas/solid flow systems: 1999 Fluor-Daniel Plenary lecture. Powder Technology 119 (2–3), 59–67.

Benyahia, S., Arastoopour, H., Knowlton, T.M., Massah, H., 2000. Simulation of particles and gas flow behaviour in the riser section of a circulating fluidized bed using the kinetic theory approach for the particulate phase. Powder Technology 112 (1–2), 24–33.

Cheng, Y., Wei, F., Yang, G.Q., Jin, Y., 1998. Inlet and outlet effects on flow patterns in gas–solid risers. Powder Technology 98 (2), 151–156.

Cheng, Y., Guo, Y., Wei, F., Jin, Y., Lin, W., 1999. Modeling the hydrodynamics of Downer reactors based on the kinetic theory. Chemical Engineering Science (54), 2019–2027.

Das, A.K., De Wilde, J., Heynderickx, G.J., Marin, G.B., Iversen, S.B., Felsvang, K., 2001. The simultaneous adsorption of SO_2–NO_x from industrial flue gases in a riser configuration. A.I.Ch.E. Journal 47, 2833–2846.

Das, A.K., Baudrez, E., Marin, G.B., Heynderickx, G.J., 2003. Three-dimensional Simulation of a Fluid Catalytic Cracking Riser Reactor. Industrial Engineering and Chemistry Research 42 (12), 2602–2617.

De Wilde, J., 2000. Adsorption of SO_2 and NO_x in a Riser: Kinetics and 3D gas–solid hydrodynamics. Ph.D. Dissertation, Universiteit Gent, Gent, Belgium.

De Wilde, J., Marin, G.B., Heynderickx, G.J., 2003a. The effects of abrupt T-outlets in a riser: 3D simulation using the kinetic theory of granular flow. Chemical Engineering Science 58, 877–885.

De Wilde, J., Van engelandt, G., Heynderickx, G.J., Marin, G.B., 2003b. Gas–solids mixing in the inlet zone of a circulating fluidized bed. Proceedings of the 2003 Annual Meeting A.I.Ch.E. November 16–21, San Francisco Hilton & Towers, San Francisco, USA.

De Wilde, J., Van engelandt, G., Heynderickx, G.J., Marin, G.B., 2005. Gas–solids mixing in the inlet zone of a dilute circulating fluidized bed. Powder Technology 151 (1–3), 96–116.

Heynderickx, G.J., Das, A.K., De Wilde, J., Marin, G.B., 2004. Effect of clustering on gas–solid drag in dilute two-phase flow. Industrial Engineering and Chemistry Research 43 (16), 4635–4646.

Knowlton, T.M., Geldart, D., Master, J., King, D., 1995. Comparison of CFB Hydrodynamic models. PSRI Challenge Problem. Eighth International Fluidization Conference, Tours, France.

Shadle, L.J., Ludlow, J.C., Mei, J.S., Guenther, C., 2001. Circulating Fluid-Bed Technology for Advanced Power Systems. Vision 21 Program Review Meeting, 6–7 november, USA. ⟨www.netl.doe.gov/publications/proceedings/01/vision21/v21p.03.pdf⟩

Sun, B., Gidaspow, D., 1999. Computation of circulating fluidized bed riser flow for the fluidization VIII benchmark test. Industrial Engineering and Chemistry Research 38 (3), 787–792 March.

Van engelandt, G., Heynderickx, G.J., Marin, G.B., 2004. Experimental study of gas–solid flow in risers. In: Arena, U., Chirone, R., Miccio, M., Salatino, P. (Eds.), Proceedings of the Fluidization XI Conference: Present and Future for Fluidization Engineering, Engineering Conferences International, May 9–13, Isschia, Italy, p. 351.

Zhang, D.Z., VanderHeyden, W.B., 2002. The effects of mesoscale structures on the macroscopic momentum equations for two-phase flows. International Journal of Multiphase Flow 28 (5), 805–822.

Zheng, Y., Wan, X., Qian, Z., Wei, F., Jin, Y., 2001. Numerical simulation of the gas-particle turbulent flow in riser reactor based on k-ε-k_p-ε_p-θ two-fluid model. Chemical Engineering Science (54), 6813–6822.